Available online at www.sciencedirect.com
SCIENCE DIRECT®
Journal of Computational Physics 206 (2005) 706–726
JOURNAL OF COMPUTATIONAL PHYSICS
www.elsevier.com/locate/jcp

Numerical study of interacting particles approximation for integro-differential equations

Dan Stanescu [a,*], Dongjin Kim [a], Wojbor A. Woyczynski [b]

[a] *Institute for Scientific Computation, Department of Mathematics, University of Wyoming, UW Postal Services, Dept. 3036, 1000 East University Avenue, Laramie, WY 82071, USA*
[b] *Department of Statistics, Case Western Reserve University, Cleveland, OH 44016, USA*

Received 14 July 2004; received in revised form 3 November 2004; accepted 6 December 2004
Available online 16 February 2005

Abstract

The paper develops a numerical method based on the interacting particles approximation (propagation of chaos) for the solution of a large class of evolution problems involving the fractional Laplacian operator and a non-local quadratic-type non-linearity. Coupled stochastic differential equations driven by Lévy symmetric α-stable processes are integrated numerically using Euler's method and the solutions of the governing equations are obtained from their statistics. The method is tested on several one- and two-dimensional examples, and established analytical properties of the solutions are verified for the numerical approximates when they are available. For initial conditions that are either integrable or monotone bounded functions, it is shown that these methods represent viable tools for constructing the solution to the Cauchy problem.

1. Introduction

The solution of stochastic differential equations through computer experiments is already a well-established area of numerical analysis, and several classic texts treat this subject and related issues in depth [1–4]. For linear parabolic equations of evolution (i.e., the heat equation), a straightforward relationship can be established with the generator of Itô diffusions [5]. This in turn may be used to develop probabilistic numerical methods for the solution of such equations, pioneering work in this direction dating back at least to the

* Corresponding author. Tel.: +1 307 766 4380; fax: +1 307 766 6838.
E-mail address: stanescu@uwyo.edu (D. Stanescu).

0021-9991/$ - see front matter © 2005 Elsevier Inc. All rights reserved.
doi:10.1016/j.jcp.2004.12.023

early seventies [6]. Relatively recently, a probabilistic framework based on a general propagation of chaos result was also developed [7–9] for non-linear initial value problems of the form

$$\begin{cases} \partial_t u = \sigma^2 \Delta_\alpha u + \nabla \cdot (uB(u)), \\ u(x,0) = u_0(x) \end{cases} \tag{1}$$

or equivalently

$$\begin{cases} \partial_t v = \sigma^2 \Delta_\alpha v + \nabla_v \cdot B(v), \\ v(x,0) = v_0(x), \end{cases} \tag{2}$$

where $0 < \alpha \leqslant 2, u, v : \Omega \times [0,T] \subset \mathbb{R}^d \times \mathbb{R}^+ \to \mathbb{R}$, $\sigma > 0$, $\Delta_\alpha := -(-\Delta)^{\alpha/2}$ is the fractional (power of the) Laplacian in $\mathbb{R}^d$ defined via the Fourier transform $\mathbb{F}$

$$\mathbb{F}((-\Delta)^{\alpha/2} u)(\omega) := (|\omega|^2)^{\alpha/2} (\mathbb{F}u(\omega)), \quad \omega \in \mathbb{R}^d, \tag{3}$$

and $B(u)$ is a linear $\mathbb{R}^d$-valued integral operator with the kernel $b : \mathbb{R}^d \times \mathbb{R}^d \to \mathbb{R}^d$:

$$B(u)(x) = \int_{\mathbb{R}^d} b(x,y) u(y)\, \mathrm{d}y. \tag{4}$$

In the interacting particles approximation methods (i.e., the discrete setting for propagation of chaos), the dependent variable u in (1) is interpreted as the probability density function of the position of a system of interacting particles moving in $\mathbb{R}^d$, in direct correspondence with the interpretation of the solution of the Fokker–Planck equation [1], while v in (2) represents the corresponding cumulative distribution function. Based on this theoretical framework we present here a Monte-Carlo type numerical method for the solution of the above initial-value problems in one and two space dimensions. Our approach uses Euler's method to integrate in time the coupled system of stochastic differential equations that govern the motion of the particles. These equations are driven by Lévy symmetric α-stable processes, which revert to Wiener processes for the case of normal diffusion.

For a general setting, we will assume that $u_0(x)$ is a non-negative smooth integrable function with compact support in $\mathbb{R}^d$ and $v_0(x)$ is a non-decreasing, right-continuous and bounded function satisfying

$$0 = \lim_{x \to -\infty} v_0(x) \leqslant \lim_{x \to +\infty} v_0(x) = c < \infty.$$

In the case of classical normal diffusion ($\alpha = 2$), Eq. (1) becomes a Fokker–Planck-type parabolic equation of evolution that is encountered for a large number of phenomena. For instance, if

$$b(x,y) = c(x-y)|x-y|^{-d}$$

and $c < 0$, then (1) models the diffusion of charge carriers in electrolytes, semiconductors or plasmas interacting via Coulomb forces. If $c > 0$, it describes gravitational interaction of particles in a cloud or galaxies in a nebula.

For the Biot–Savart kernel

$$b(x,y) = (2\pi)^{-1}(x_2 - y_2, y_1 - x_1)|x-y|^{-2} \tag{5}$$

in $\mathbb{R}^2$, it becomes equivalent to the vorticity formulation of the two-dimensional Navier–Stokes equations. Also, if the kernel b is the Dirac distribution

$$b(x,y) = c\delta(x-y)$$

in $\mathbb{R}$, one obtains the one-dimensional Burgers' equation

$$\partial_t u = \sigma^2 \partial_{xx} u + c\partial_x(u^2). \tag{6}$$

Burgers' equation is also obtained if the kernel b in (2) is the Heaviside function, $b(x,y) = cH(x-y)$, where $H(z) = 0$ if $z < 0$ and $H(z) = 1$ if $z \geqslant 0$, leading to

$$\partial_t v = \sigma^2 \partial_{xx} v + cv\partial_x v. \tag{7}$$

Furthermore, for

$$b(x,y) = (c_1\delta(x-y), c_2\delta(x-y), \ldots, c_d\delta(x-y))$$

in $\mathbb{R}^d$, then (1) becomes the fractal Burgers equation

$$\partial_t u = \sigma^2 \Delta_\alpha u + c \cdot \nabla(u^2), \tag{8}$$

where $c = (c_1, c_2, \ldots, c_d) \in \mathbb{R}^d$, and if $b(x,y) = c\delta(x-y)$ in $\mathbb{R}$, Eq. (2) is the fractal Kardar–Parisi–Zhang equation governing interface growth [10]

$$\partial_t v = \sigma^2 \Delta_\alpha v + c(\partial_x v)^2. \tag{9}$$

The extension of classical parabolic equations to the fractional diffusion case is motivated by the fact that such anomalous diffusion processes are encountered in several areas of science and technology. These include non-linear acoustics, statistical mechanics, biology, fluid flow and mathematical finance. Our main interest resides in developing a numerical methodology for the modeling of phenomena related to interfacial growth in chemical vapor deposition (CVD) processes [11], which involve hopping and trapping of molecules and hence are governed by such equations. Let us note from the onset that a direct numerical approach to such equations of evolution, using for example classical techniques such as finite differences, is extremely difficult due to the doubly non-local character of the equations [7]. First, the fractional Laplacian operator $\Delta_\alpha = -(-\Delta)^{\alpha/2}$ for $\alpha \in (0,2)$ is no longer a differential but an integro-differential operator, and second, the non-linear convection term may involve integrals over the whole space $\mathbb{R}^d$. Spectral methods [12] do, however, constitute an exception to this rule, since the evaluation of the fractional Laplacian operator is straightforward in Fourier space. Similarly, the integral convolution operator $B(u)$ becomes a product in Fourier space and can be evaluated easily. The non-linear convection term appearing in the governing equations is, on the other hand, usually computed by what is known as a pseudospectral approach. This involves transforming from Fourier to physical space, evaluating the non-linearity in physical space, then transforming back to Fourier space. A well-known problem with this approach is the introduction of an aliasing error [12]. Also, the initial data for the CVD processes we are interested in is not periodic. Instead, the initial surface height is a random variable for which we may know, at most, some statistical measures (i.e., the first moment and second moment). While the use of spectral methods remains an alternative, the above reasons together with the current lack of expertise in the use of probabilistic methods for fractional diffusion problems (to the authors' knowledge, the only numerical work to date was for the case of normal diffusion [13,14]) render the latter worth studying. While more demanding than Fourier spectral methods in terms of computing resources, in particular in fewer space dimensions, their better understanding is crucial to the development of more cost-effective strategies, for example the use of importance sampling. Finally, we would like to note that the interacting particles method also offers promise for boundary value problems involving the fractional Laplacian.

The paper is arranged as follows: in the next section we describe the interacting particles approximation and present several asymptotic properties of the solutions to the governing equations which we need to validate our results. Section 3 is devoted to an algorithmic discussion of our implementation. Numerical experiments for several problems with various initial conditions for one and two space dimensions are reported in the next two sections.

In terms of notation, throughout this paper we use $\|u\|_p$ for the norm in $L^p(\mathbb{R}^d)$ and H^β for the usual Sobolev space $W^{\beta,2}(\mathbb{R}^d)$. Any constant independent of solutions is denoted by c.

2. The interacting particles approximation

We assume that $\alpha \in (1,2]$ which allows us to operate with expectations of the corresponding α-stable processes [9] and restrict most of the subsequent discussion to Eq. (1) for simplicity, since the extension to Eq. (2) is relatively straightforward. Let $u = u(x,t) \geqslant 0$, $x \in \mathbb{R}^d$, $t \in (0,T)$ be a local in time weak solution of the initial-value problem (1) with kernel $b(x,y) = b(x-y)$ satisfying potential estimates of the type

$$|b(x)| \leqslant c_1|x|^{\beta_1-d} \quad \text{or} \quad |\nabla b(x)| \leqslant c_2|x|^{\beta_2-d} \tag{10}$$

for some $0 < \beta_1, \beta_2 < d$ and $0 < c_1, c_2$. Here, a weak solution is a function $u \in L^2((0,T);\ H^{\alpha/2}(\mathbb{R}^d))$ such that the integral identity

$$\int_{\mathbb{R}^d} u\eta \,\mathrm{d}x - \int_0^t \mathrm{d}s \int_{\mathbb{R}^d} u\eta_s \,\mathrm{d}x + \int_0^t \mathrm{d}s \int_{\mathbb{R}^d} (\Delta_{\alpha/2} u \Delta_{\alpha/2}\eta + uB(u)\cdot\nabla\eta)\,\mathrm{d}x = \int_{\mathbb{R}^d} u_0(x)\eta(x,0)\,\mathrm{d}x$$

holds for every test function $\eta \in H^1((0,T)\times\mathbb{R}^d)$. For an initial condition $0 \leqslant u_0 \in L^2(\mathbb{R}^d)\cap L^1(\mathbb{R}^d)$, local and global existence results for such weak solutions have been established in [9].

Without loss of generality we may assume that u is bounded, i.e.

$$\sup_{x\in\mathbb{R}^d, t\in[0,T]} |u(x,t)| < \infty. \tag{11}$$

Moreover, since we will be working with $(L^1\cap L^\infty)$-solutions, the estimate

$$\sup_{x\in\mathbb{R}^d, t\in[0,T]} |B(u)(x)| < \infty \tag{12}$$

follows from the potential estimate (10), the Sobolev embedding theorem, and the boundedness of the solution u.

Consider a solution X_t of the stochastic differential equation

$$\begin{cases} \mathrm{d}X_t = \sigma\,\mathrm{d}S_t - B(u)(X_t)\,\mathrm{d}t, \\ X_{t=0} = X_0, \quad X_0 \sim u_0(x)\,\mathrm{d}x, \end{cases} \tag{13}$$

where $t \in [0,T]$, S_t is a standard symmetric α-stable process with its values in $\mathbb{R}^d$. Since the coefficient $B(u)(X_t)$ in (13) is bounded, this stochastic differential equation has a unique weak solution. Furthermore, the stochastic process X_t is related to a solution u of (1) satisfying (11) by

$$P(X_t \in \mathrm{d}x) = u(x,t)\,\mathrm{d}x.$$

In other words X_t is the non-linear Markov process corresponding to this evolution equation (we refer to [9] for the proof). For Eq. (2) the corresponding relation is

$$P(X_t \leqslant x) = v(x,t)$$

with $v_0(x) = v(x,0)$ the cumulative distribution function of the random variable X_0.

The interacting particles approximation constructs the above solutions in a statistical way using a Monte-Carlo simulation approach. To describe it, let $\{S_t^i\}_{i=1,2,\ldots,N}$ be N independent copies of Lévy symmetric α-stable processes with the common infinitesimal generator $\Delta_\alpha = -(-\Delta)^{\alpha/2}$. When $\alpha = 2$, the case of normal diffusion, S_t^i becomes the familiar Wiener process (Brownian motion). The approximation has been studied extensively, both analytically and numerically [13–16], in the case when the driving process is a Wiener process. Propagation of chaos results for Lévy symmetric α-stable processes [7] have been obtained recently by regularizing the corresponding stochastic differential equations (see Eq. (15) below) because of the weak parabolic regularization effect of Δ_α. Therefore, let $\delta_\epsilon(x) := (2\pi\epsilon)^{-d/2}\exp(-|x|^2/(2\epsilon))$, $\epsilon > 0$, be a standard smoothing kernel.

Consider the measure-valued process (empirical distribution)

$$Y_t^{N,\epsilon} := \frac{1}{N}\sum_{i=1}^{N}\delta(X_t^{i,N,\epsilon}) \tag{14}$$

of N interacting particles with positions $\{X_t^i\}_{i=1,\ldots,N} := \{X_t^{i,N,\epsilon}\}_{i=1,\ldots,N}$, whose dynamics is described by the system of regularized stochastic differential equations

$$\mathrm{d}X_t^i = \sigma\,\mathrm{d}S_t^i - \frac{1}{N}\sum_{j\neq i} b_\epsilon(X_t^i - X_t^j)\,\mathrm{d}t, \quad i = 1,\ldots,N, \tag{15}$$

where $b_\epsilon = \delta_\epsilon * b$.

Assume that the initial particles' positions $\{X_0^i\}_{i=1,\ldots,N}$ satisfy

$$\sup_N \sup_{\lambda\in\mathbb{R}^d} \frac{N^{1-1/\alpha}}{1+|\lambda|^a} E\left[\left\langle Y_0^{N,\epsilon} - u_0^\epsilon(x), \mathscr{X}\lambda\right\rangle\right] < \infty \tag{16}$$

for some $a \geqslant 0$ and all the characters $\mathscr{X}\lambda(x) = \mathrm{e}^{\mathrm{i}\lambda x}$. Then, for each $\epsilon > 0$, the empirical process $Y_t^{N,\epsilon}$ is weakly convergent

$$Y_t^{N,\epsilon} \Rightarrow u^\epsilon(x,t)\,\mathrm{d}x \quad \text{in probability as } N\to\infty, \tag{17}$$

where $\Rightarrow$ denotes the weak convergence of measures, and the limit density $u^\epsilon := \mathrm{u}^\epsilon(x,t)$, $x\in\mathbb{R}^d$, $t\in[0,T]$, satisfies the regularized equation

$$\partial_t u^\epsilon = \sigma^2 \Delta_\alpha u^\epsilon + \nabla\cdot(u^\epsilon B_\epsilon(u^\epsilon)) \tag{18}$$

with $B_\epsilon = \delta_\epsilon * B$.

Furthermore, given any sequence of regularizations (18) with $\epsilon\to 0$, the family of empirical distributions $\{Y_t^{N,\epsilon}\}$ contains a sub-sequence weakly convergent to a solution $u(x,t)$ of (1) [7]. Thus, if u^ϵ are solutions of the regularized Eq. (18) such that their initial conditions satisfy $\|u^\epsilon - u_0\|_2 \to 0$ as $\epsilon\to 0$ for some $u_0\in L^2(\mathbb{R}^d)$, then given any sequence $\epsilon_k\to 0$ as $k\to 0$, there exists a sequence $N_k\to\infty$ and a weak solution $u(x,t)$ of (1) such that for each $\phi\in C_0^\infty(\mathbb{R}^d)$ and all $t\in[0,T]$

$$E\left[\left\langle Y_t^{N_k,\epsilon_k} - u(x,t), \phi(x)\right\rangle\right] \to 0 \quad \text{as} \quad N_k\to\infty.$$

We note that the solution $v(x,t)$ to (2) at a fixed time t can be similarly approximated by the following measure-valued process:

$$Z_t^{N,\epsilon}(x) := \frac{1}{N}\sum_{i=1}^{N} H(x - X_t^{i,N,\epsilon}) \quad \forall x\in\mathbb{R}^d. \tag{19}$$

Regarding the convergence of the approximation, the following was proven in a general setting by Bossy and Talay [15] for the case of normal diffusion:

Convergence rate. *For T fixed, let $\Delta t > 0$ be such that $T = L\Delta t$, $L\in\mathbb{N}$. Let $v(x,t_k)$ be the solution at time $t_k = k\Delta t$ of Burgers' equation (7) with the initial condition v_0. Let $V(x,t_k)$ be the interacting particles approximation, with the number of particles denoted by N. There exists a strictly positive constant c depending on σ, v_0 and T such that, for all $k = 1, 2,\ldots,L$*

$$E\|v(\cdot,t_k) - V(\cdot,t_k)\|_1 \leqslant c\left(\frac{1}{\sqrt{N}} + \sqrt{\Delta t}\right). \tag{20}$$

The time discretization error in the above estimate comes from the Euler discretization. For additive noise as in Eq. (15), the case we are interested in, the above estimate is not sharp; Euler's method has strong order

one in this case (i.e., the error is proportional to Δt). Both the numerical results presented in [15] and our results in the later sections confirm this latter fact. Unfortunately, the fractional diffusion case is far more complicated and so far we could not obtain an analytical result for the convergence rate of the interacting particles approximation (note however the results of Jacod [17] and Protter and Talay [18] for Euler's method in the context of Lévy processes). We propose the following conjecture fully supported by our numerical results as shown in the subsequent sections:

Convergence rate for additive noise. *For T fixed, let $\Delta t > 0$ be such that $T = L\Delta t,\ L \in \mathbb{N}$. Let $v(x, t_k)$ be the solution at time $t_k = k\Delta t$ of Eq. (8) with $\alpha \in (1, 2]$ and initial condition v_0. Let $V(x, t_k)$ be the interacting particles approximation, with the number of particles denoted by N. There exists a strictly positive constant c depending on σ, v_0 and T such that, for all $k = 1, 2, \ldots, L$*

$$E\|v(\cdot, t_k) - V(\cdot, t_k)\|_1 \leqslant c\left(\frac{1}{\sqrt{N}} + \Delta t\right). \tag{21}$$

3. Algorithm description

In this section, we illustrate in detail the algorithm for the numerical solution of the initial-value problems (1) and (2), based upon the time discretization of the system of regularized stochastic differential equation (15).

To solve the system (15) numerically, we first discretize the time interval $[0, T]$. Although a fixed time step is not needed, for simplicity we let $\Delta t = T/L$ for some positive integer L, and $t_k = k\Delta t$, $k = 1, 2, \ldots, L$. Our numerical approximation to X_{t_k} and S_{t_k} will be denoted X_k and S_k, respectively. The explicit Euler scheme leads to the following discrete-time system: for $1 \leqslant i \leqslant N$ and $1 \leqslant k \leqslant L$

$$X_k^i = X_{k-1}^i + \sigma\left(S_k^i - S_{k-1}^i\right) - \frac{1}{N}\sum_{j \neq i} b_\epsilon\left(X_{k-1}^i - X_{k-1}^j\right)\Delta t, \tag{22}$$

$$X_0^i = x_0^i, \tag{23}$$

where the N initial particles $\{x_0^i\}_{i=1,\ldots,N} \subset \mathbb{R}^d$ are independent random numbers whose probability density is given by the initial condition u_0 in (1).

For the generation of the time increments of the Lévy symmetric α-stable processes $\{S^i\}_{i=1,\ldots,N}$, several methods are available [19–21]. While the algorithm due to Chambers et al. [21] allows the generation of general Lévy distributions, for the restricted case of symmetrically stable processes we chose the fast algorithm due to Mantegna [20]. It allows us to generate the time increments for any index α ranging continuously from 0.3 to 1.99. We briefly outline the algorithm below. For the case $\alpha = 2$, a normal distribution random number generator is used instead [2].

Mantegna's algorithm uses a fitted asymptotic expansion for the generation of stable distributions. The first step in this algorithm is to generate a set of independent random variables of the form

$$s_i = \frac{x_i}{|y_i|^{1/\alpha}}, \quad i = 1, \ldots, m, \tag{24}$$

where x_i and y_i are two random variables normally distributed with standard deviation σ_x and σ_y, respectively. The stochastic variable

$$z_m = \frac{1}{m^{1/\alpha}}\sum_{i=1}^{m} w_i, \tag{25}$$

where m independent stochastic variables $\{w_i\}_{i=1,2,\ldots,m}$ are generated independently from random variables s_i by

$$w_i = [(K(\alpha)-1)\exp(-|s_i|/C(\alpha))+1]s_i, \quad i = 1,\ldots,m \tag{26}$$

converges very fast to a symmetric α-stable distribution. Here the two parameters $K(\alpha)$ and $C(\alpha)$ are obtained by fitting the asymptotic expansion of the Lévy distribution such that it holds both for large and small absolute values of the argument.

The final solution stage involves constructing a histogram from the particle positions to compute the empirical distributions (14) and (19) that approximate the solutions $u(x,t)$ of (1) and $v(x,t)$ of (2), respectively.

4. Numerical experiments in one space dimension

In this section several initial-value problems of the form (1) and (2) both with normal diffusion ($\alpha = 2$) and anomalous diffusion ($1 < \alpha < 2$) are solved using the interacting particles approximation. Since normal diffusion has been studied previously by other researchers [13–15], results for $\alpha = 2$ are presented here only for validation and comparison purposes, as in this case some of the problems that we consider have an analytical solution.

4.1. Integrable initial conditions

A natural setting for the methods discussed herein arises when the initial conditions are integrable functions. Such initial conditions can in turn be interpreted as probability density functions of the particle positions at time $t = 0$. Thus, the first problem considered is

$$\begin{cases} \partial_t u + u\partial_x u = \sigma^2 \Delta_\alpha u, \quad 1 < \alpha \leqslant 2, \\ u(x,0) = 1/\sqrt{2\pi}\exp(-x^2/2), \end{cases} \tag{27}$$

where $u = u(x,t)$, $x \in \mathbb{R}$, and $t \in [0,T]$. This initial-value problem is obtained from (1) by taking $b(x,y) = -1/2\delta(x-y)$, and $d = 1$ where $\delta(x)$ is the Dirac distribution. Computations have been performed for two different diffusion coefficients, $\sigma^2 = 1$ and $\sigma^2 = 0.01$, respectively. The discrete-time system of regularized stochastic differential equations becomes

$$X_k^i = X_{k-1}^i + \sigma(S_k^i - S_{k-1}^i) + \frac{1}{2N}\sum_{j\neq i}\delta_\epsilon(X_{k-1}^i - X_{k-1}^j)\Delta t, \tag{28}$$

$$X_0^i = x_0^i \tag{29}$$

for $1 \leqslant i \leqslant N$ and $1 \leqslant k \leqslant L$; $\{S^i\}_{i=1,\ldots,N}$ are independent Lévy symmetric α-stable processes.

When $\alpha = 2$, Eq. (27) becomes the one-dimensional classical Burgers' equation for which the well-known Cole–Hopf transformation provides the analytical solution

$$u(x,t) = \frac{\int_{-\infty}^{\infty}[(x-y)/t]\exp[(2\sigma^2)^{-1}(\xi(y)-(x-y)^2/2t)]\,\mathrm{d}y}{\int_{-\infty}^{\infty}\exp[(2\sigma^2)^{-1}(\xi(y)-(x-y)^2/2t)]\,\mathrm{d}y}, \tag{30}$$

where $\xi(x) = -\int_{-\infty}^{x} u(y,0)\,\mathrm{d}y$. For the numerical approximation we generated an approximate initial condition by sampling from a standard normal pseudo-random number generator. Fig. 1 compares the interacting particles approximation obtained using this approximate initial condition to the analytical

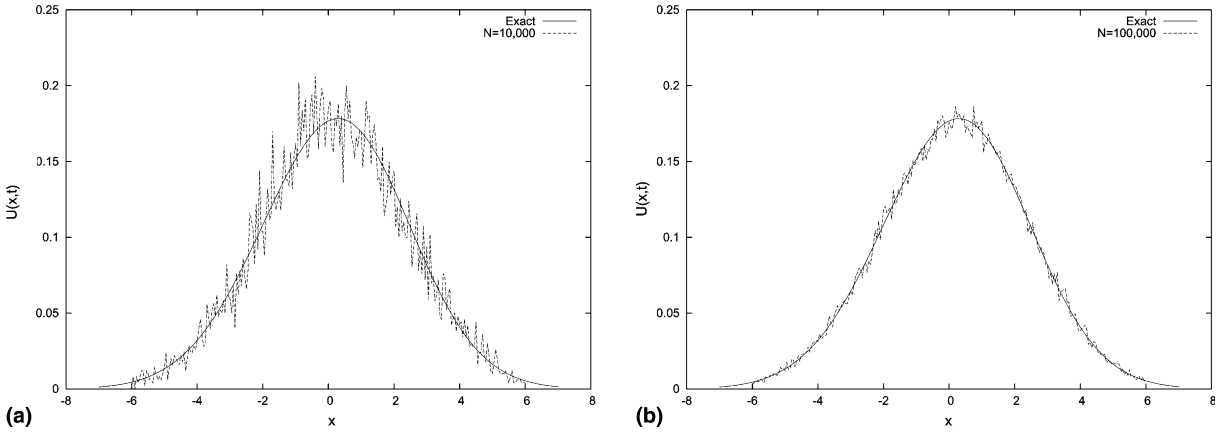

Fig. 1. Interacting particles approximation to the solution of the 1D Burgers' equation with $\sigma^2 = 1$ at time $T = 2$ using (a) 10,000 particles (b) 100,000 particles. Smoothing parameter $\epsilon = 1.0$. Exact solution also shown (full line).

solution of the one-dimensional Burgers' equation with viscosity $\sigma^2 = 1$ at time $T = 2$ using 10,000 and 100,000 samples, respectively.

For $1 < \alpha < 2$, the initial-value problem (27) becomes the one-dimensional fractal Burgers' equation. Results are presented in this case for two different indices of stability, $\alpha = 1.5$ and 1.25. Figs. 2 and 3 show the time evolution of the solution of (27) for the case $\sigma^2 = 1$, $\alpha = 1.5$ and $\sigma^2 = 0.01$, $\alpha = 1.25$ compared to the case $\alpha = 2$, respectively. The first case corresponds to a solution dominated by diffusion and the latter to a solution dominated by convective effects. The effect of the smoothing parameter ϵ appearing in the regularizing kernel δ_ϵ is captured in Fig. 4 for two different values of viscosity, $\sigma^2 = 1$ and $\sigma^2 = 0.01$. As it may be expected, the effect is large for the convection-dominated case and negligible for the diffusion-dominated case. In all numerical experiments we conducted so far we did not notice any negative effect when assigning a very small value to the smoothing parameter ($\epsilon = 0.0001$), which obviously represents a safe practice for convection-dominated problems.

To further validate our numerical experiments for the anomalous diffusion case, we consider the following property of the solutions to the fractal Burgers' equation, see [7] for details:

Time decay of solutions: *Let* $0 < \alpha \leqslant 2$. *Suppose u is a sufficiently regular solution of the* (*multidimensional*) *fractal Burgers' equation* (8) *with* $u_0 \in L^1(\mathbb{R}^d)$. *Then the* L^2*-norm of u decays, as* $t \to \infty$, *at a rate given by*

$$\|u(t)\|_2 \leqslant c(1+t)^{-d/(2\alpha)}. \tag{31}$$

Table 1 presents estimates of the discrete L^2-norm of the approximate solution $U(x, T)$ for $\sigma = 1$, $\sigma = 1.5$ at times $T = 1, 2, \ldots, 5$. The discrete L^2-norm is computed here as

$$\|U\|_2 = \sqrt{\sum_{j=1}^{M} U^2(x_j, T)}, \tag{32}$$

where $-10 = x_1 < x_2 < \cdots < x_{M-1} < x_M = 10$, $M = 201$. Numerically, we obtain the following inequality:

$$\|U(t)\|_2 \leqslant 1.5215(1+t)^{-1/3}.$$

We plot the analytical estimates for the decay rate versus the numerical results for this case alongside the normal diffusion case in Fig. 5.

4.2. Bounded initial conditions

In this subsection we solve the initial-value problem

$$\begin{cases} \partial_t v - v\partial_x v = \Delta_\alpha v, \quad 1 < \alpha \leqslant 2, \\ v(x,0) = \frac{1}{2}(\tanh(x/4) + 1), \end{cases} \tag{33}$$

where $v = v(x,t)$, $x \in \mathbb{R}$, and $t \in [0,T]$. This initial-value problem is an example of (2) obtained by taking $b(x,y) = H(x-y)$, $\sigma = 1$, and $d = 1$ where $H(x)$ is the Heaviside function. As mentioned in Section 2, we

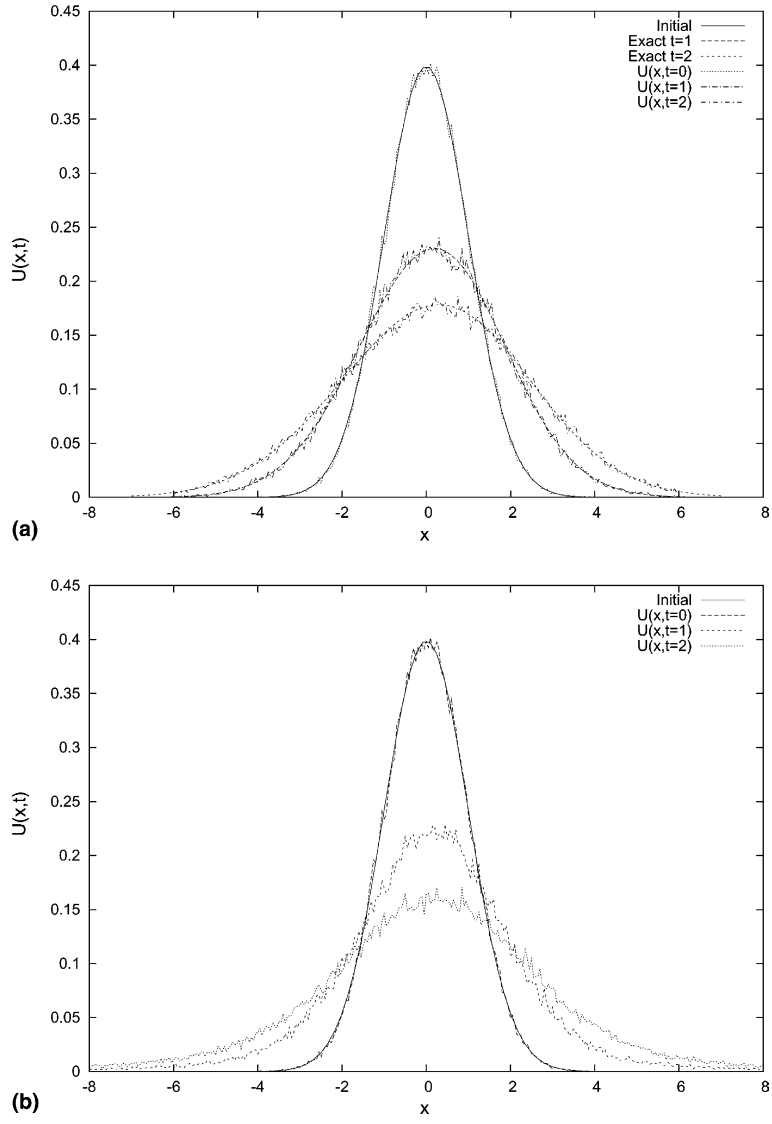

Fig. 2. Approximate solution for the 1D Burgers' equation with $\sigma^2 = 1$ using 100,000 particles with smoothing parameter $\epsilon = 1$ at $t = 0$, 1, 2 (a) 1D classical Burgers' equation ($\alpha = 2$), exact solution also shown (full line) (b) 1D fractal Burgers' equation ($\alpha = 1.5$).

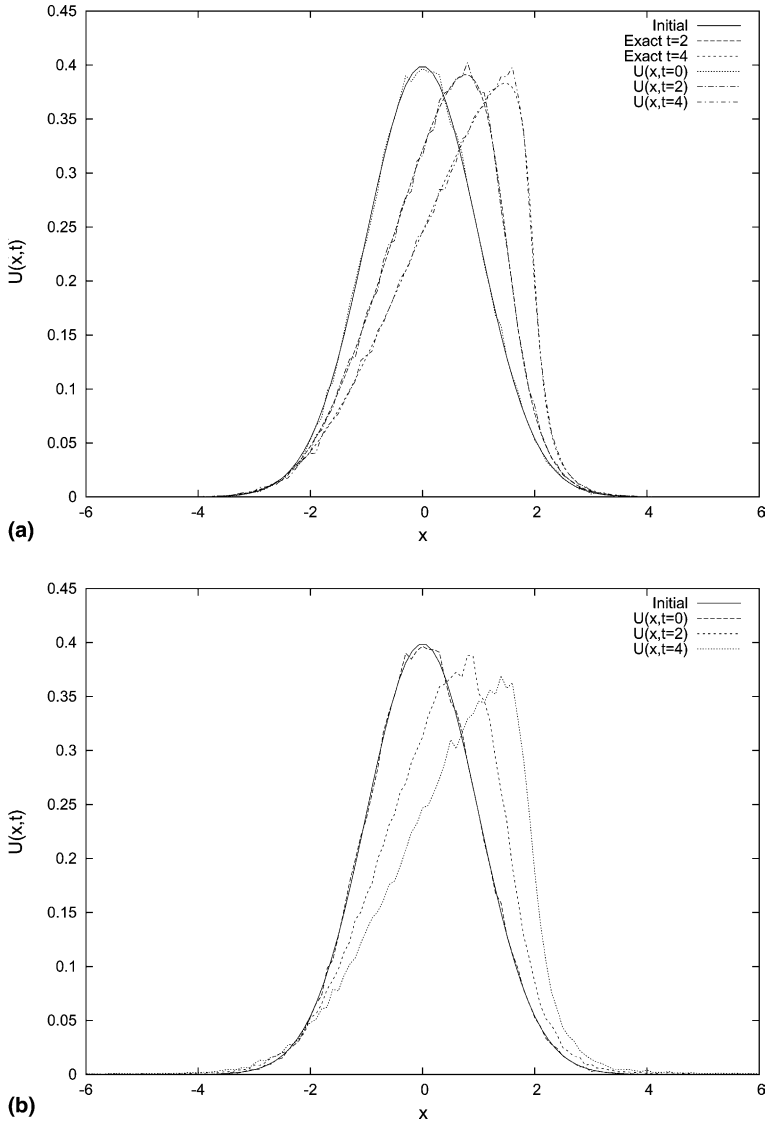

Fig. 3. Approximate solution for the 1D Burgers' equation with $\sigma^2 = 0.01$ using 100,000 particles with smoothing parameter $\epsilon = 0.01$ at $t = 0, 2, 4$ (a) 1D classical Burgers' equation ($\alpha = 2$), exact solution also shown (full line) (b) 1D fractal Burgers' equation ($\alpha = 1.25$).

interpret the solution of Eq. (33) as the cumulative distribution function of a system of particles whose probability density function satisfies the following equation:

$$\begin{cases} \partial_t u = \Delta_\alpha u + \partial_x (u \int_{\mathbb{R}} H(x-y) u(y,t)\,\mathrm{d}y), \quad 1 < \alpha \leqslant 2, \\ u(x,0) = u_0(x), \end{cases} \tag{34}$$

where $u_0(x) = \partial_x v(x,0) = \partial_x [\frac{1}{2}(\tanh(x/4) + 1)]$.

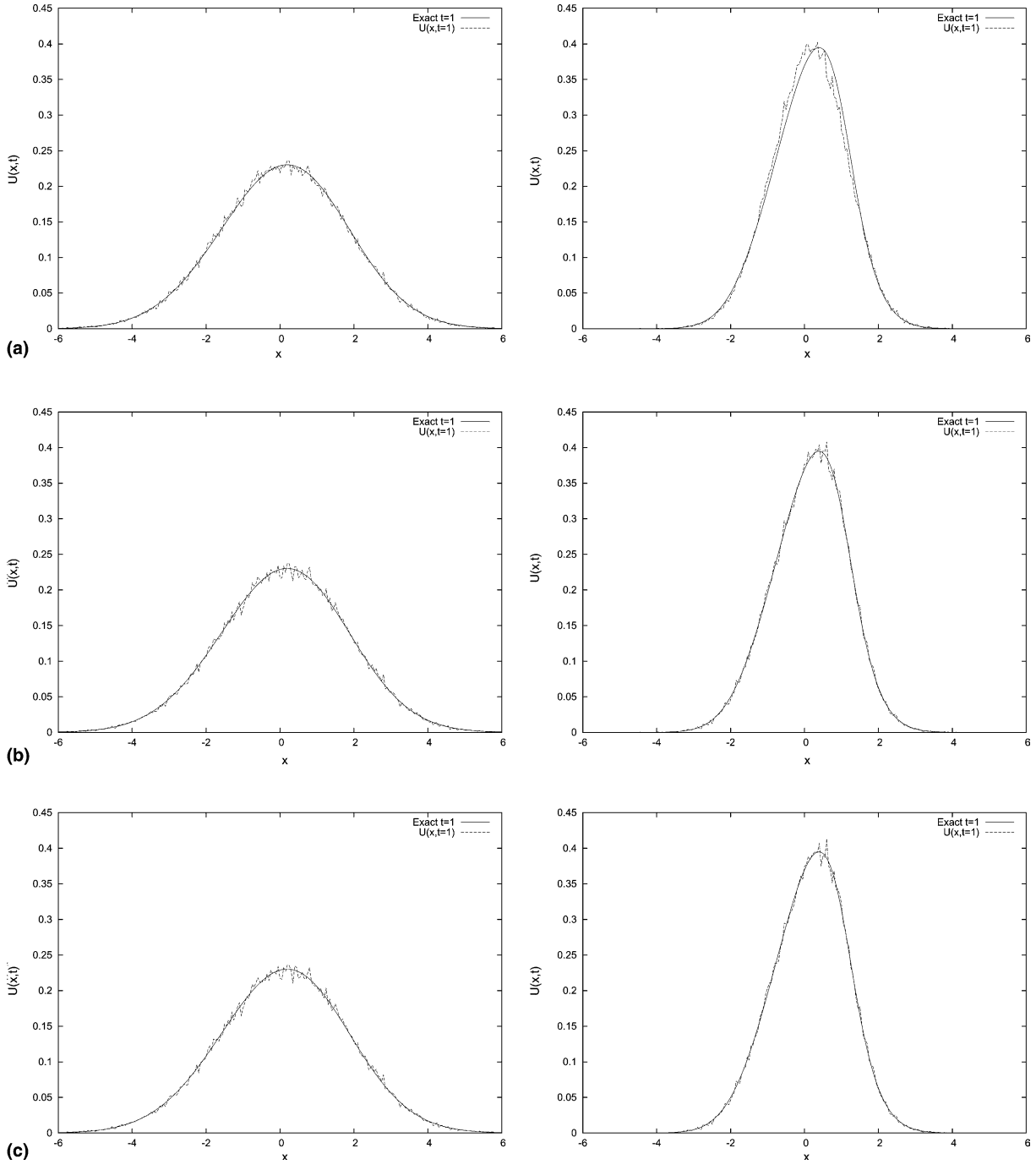

Fig. 4. Effect of the smoothing parameter ϵ in the regularizing kernel for $N = 100{,}000$ particles for $\sigma^2 = 1$ left column) and $\sigma^2 = 0.01$ (right column). Exact solution also shown (full line). (a) $\epsilon = 1$ (b) $\epsilon = 0.01$ (c) $\epsilon = 0.0001$.

Table 1
Time decay of the solution of 1D fractal Burgers' equation ($\alpha = 1.5$)

T	1	2	3	4	5
$\|U\|_2$ ($N = 10{,}000$)	1.210	1.024	0.909	0.847	0.788
$\|U\|_2$ ($N = 50{,}000$)	1.208	1.014	0.907	0.828	0.772

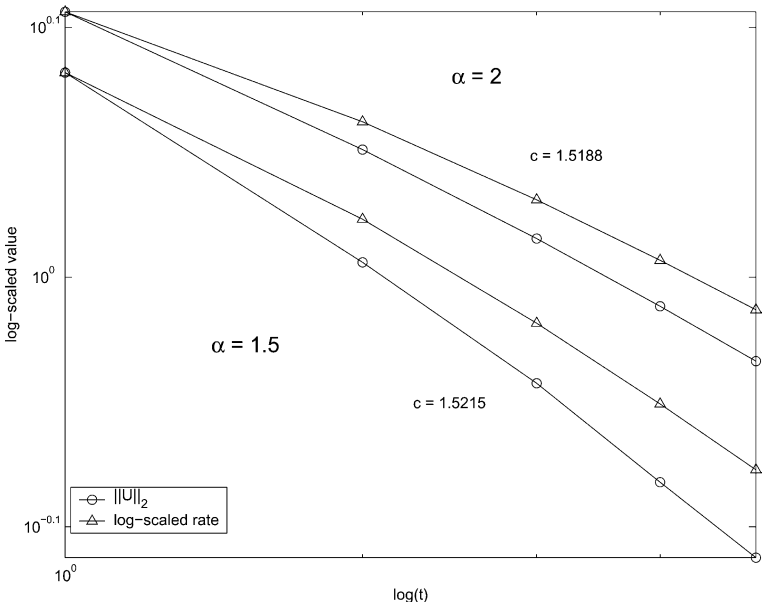

Fig. 5. Time decay of solution to the classical ($\alpha = 2$) Burgers' equation (curves above) and 1D fractal ($\alpha = 1.5$) Burgers' equation (curves below) computed using 50,000 particles. Also shown are the estimated values of the constant c in (31).

The corresponding system of regularized stochastic differential equations is given by

$$X_k^i = X_{k-1}^i + (S_k^i - S_{k-1}^i) - \frac{1}{N}\sum_{j\neq i} H_\epsilon(X_{k-1}^i - X_{k-1}^j)\Delta t, \tag{35}$$

$$X_0^i = x_0^i. \tag{36}$$

The inverse transform method [2] is used to generate pseudo-random numbers for the initial positions $\{x_0^i\}_{i=1,\ldots,N}$ in the discrete system (35) and (36), since the initial distribution function $v(x,0)$ in (33) is invertible.

For $\alpha = 2$, Eq. (33) becomes the one-dimensional classical Burgers' equation in a changed frame of reference. The solution is a traveling wave of the form

$$v(x,t) = \tfrac{1}{2}(\tanh((x + t/2)/4)) + 1). \tag{37}$$

Fig. 6 shows this solution at three time instants, $t = 0, 1, 2$. We further use this known solution to study the convergence rate of the interacting particles approximation, by computing an approximation of the L^1-norm of the error at time T

$$\|\text{error}\|_1 = \|v(\cdot,T) - V(\cdot,T)\|_1 \simeq \sum_{j=1}^{M} |v(x_j,T) - V(x_j,T)|\Delta x, \tag{38}$$

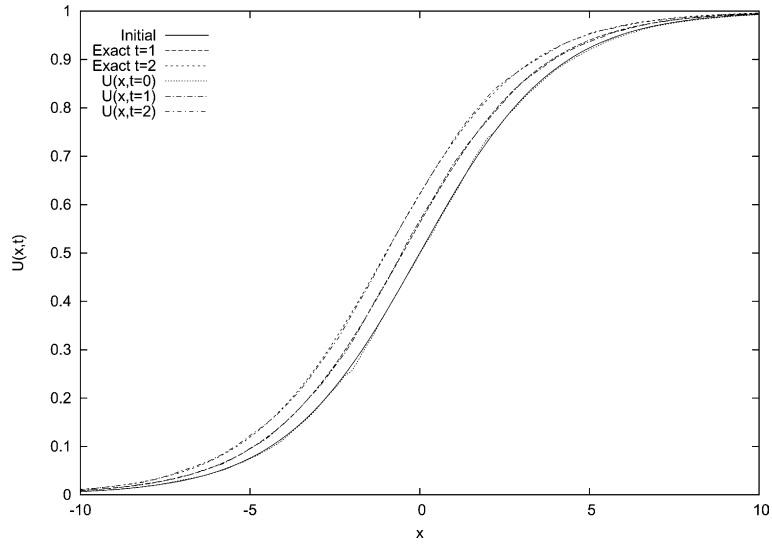

Fig. 6. Interacting particles approximation to the 1D classical Burgers' equation ($\alpha = 2$). $N = 10{,}000$ and $t = 0, 1, 2$. Exact solution also shown (full line).

where $\{x_j\}_{j=1}^{M}$ represents the equidistant (with step size Δx) discretization of the spatial domain used to construct the empirical measure (histogram). The expectation of the L^1-norm of the error is computed by averaging computations based on different initializations of the pseudo-random number generator.

Tables 2 and 3 show the results corresponding to $N = 500 \times 2^l$ and $\Delta t = 2^{-l}$ for $l = 1, \ldots, 5$, respectively. These results are representative of results we obtained for a number of test cases. The slopes of the linear interpolant obtained by a least squares fit to the data indicate an error satisfying

$$E\|v(\cdot, t_k) - V(\cdot, t_k)\|_1 = \mathrm{O}(N^{-1/2} + \Delta t). \tag{39}$$

In the case of anomalous diffusion, the solution behavior is different from the case of normal diffusion; that is, while the solution of the classical Burgers' equation propagates without deformation, the solution of the fractal Burgers' equation expands while propagating. Fig. 7 shows the shape of the solution of the initial-value problem (33) at the same three time instants for $\alpha = 1.5$. Tables 4 and 5 present our numerical results for the convergence to the exact solution as a function of N and Δt. These results are also plotted in Figs. 8 and 9. Since no exact solution is known in this case, we constructed it numerically using $N = 300{,}000$ particles and $\Delta t = 0.001$.

4.3. Fractal Burgers-KPZ equations

We consider next the one-dimensional fractal KPZ equation with a bounded function as an initial condition,

Table 2
Convergence rate versus N for $\Delta t = 0.001$ fixed

N	1000	2000	4000	8000	16,000
$E\|\text{error}\|_1$	2.8138e − 2	2.0669e − 2	1.3203e − 2	9.4255e − 3	6.6555e − 3

Table 3
Convergence rate versus Δt for $N = 100{,}000$ fixed

Δt	1/2	1/4	1/8	1/16	1/32
$E\|\text{error}\|_1$	3.0222e − 1	1.5006e − 1	7.5150e − 2	3.7756e − 2	1.9148e − 2

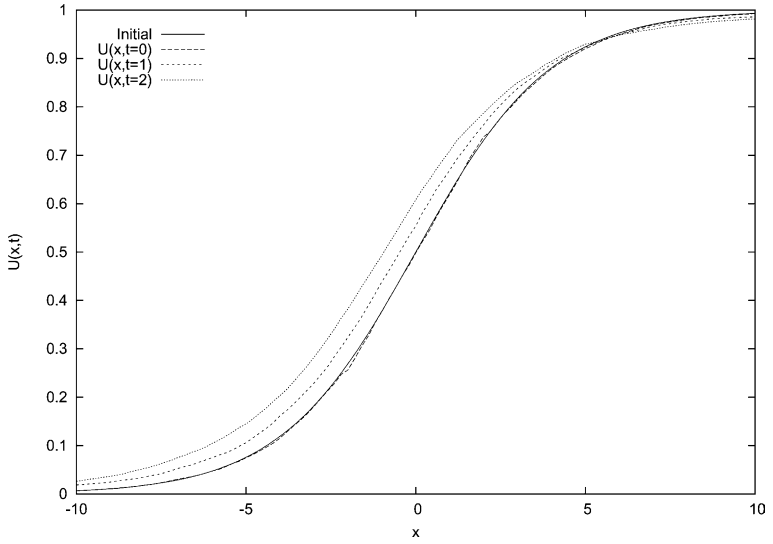

Fig. 7. Interacting particles approximation to the 1D fractal Burgers' equation ($\alpha = 1.5$). $N = 10{,}000$ and $t = 0, 1, 2$.

Table 4
Convergence rate versus N for $\Delta t = 0.005$ fixed

N		2000	4000	8000	16,000
$E\|\text{error}\|_1$	$\alpha = 1.5$	3.8131e − 2	2.1395e − 2	1.3986e − 2	1.1831e − 2
	$\alpha = 1.25$	4.2994e − 2	2.5262e − 2	1.6873e − 2	1.3023e − 2

Table 5
Convergence rate versus Δt for $N = 100{,}000$ fixed

Δt		1/4	1/8	1/16	1/32
$E\|\text{error}\|_1$	$\alpha = 1.5$	1.4005e − 1	6.6693e − 2	2.9792e − 2	1.4254e − 2
	$\alpha = 1.25$	1.3460e − 1	6.2899e − 2	2.7638e − 2	1.4305e − 2

$$\begin{cases} \partial_t v + (\partial_x v)^2 = \Lambda_\alpha v, \quad 1 < \alpha \leqslant 2, \\ v(x,0) = \frac{1}{2}(\tanh(x) + 1), \end{cases} \tag{40}$$

where $v = v(x,t)$, $x \in \mathbb{R}$, and $t \in [0,T]$. This initial-value problem can be obtained from (2) by taking the potential kernel $b(x,y) = -\delta(x-y)$, $\sigma = 1$, and $d = 1$. One can also interpret the solution to Eq. (40) as the cumulative distribution function of a system of particles whose probability density function is a solution to the following PDE:

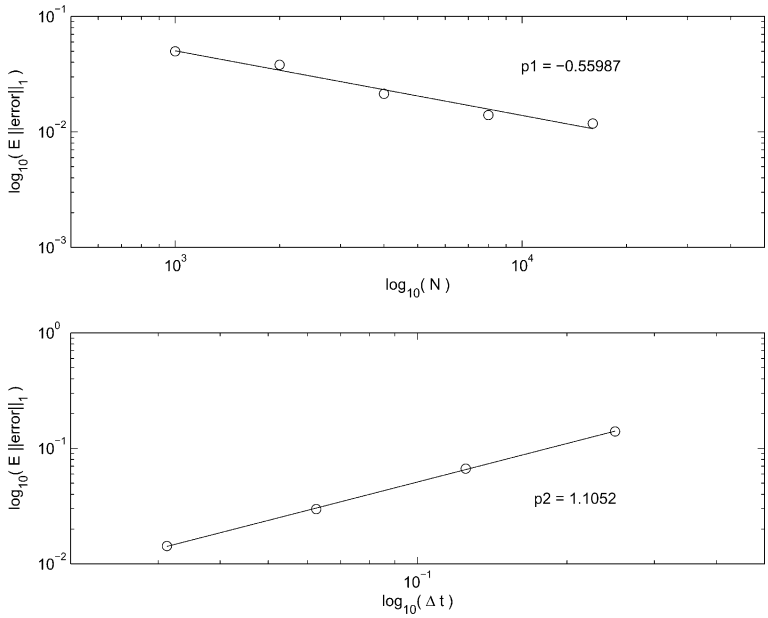

Fig. 8. Expectation of the L^1-norm of the error for $\alpha = 1.5$ as a function of the number of particles N (top) and of the time step Δt (bottom). $p1$ and $p2$ represent the least-square fits of the exponents in the error bound $E\|\text{error}\|_1 = \mathrm{O}(N^{p1} + \Delta t^{p2})$.

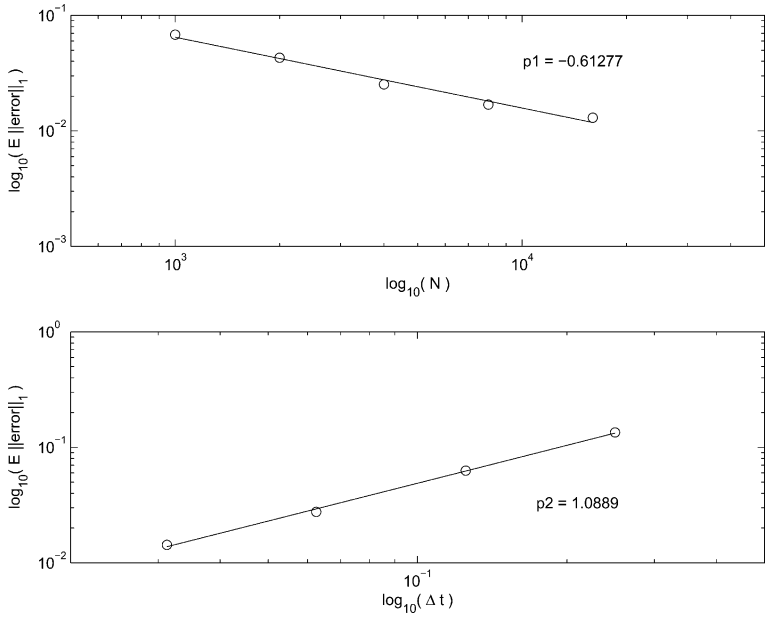

Fig. 9. Expectation of the L^1-norm of the error for $\alpha = 1.25$ as a function of the number of particles N (top) and of the time step Δt (bottom). $p1$ and $p2$ represent the least-square fits of the exponents in the error bound $E\|\text{error}\|_1 = \mathrm{O}(N^{p1} + \Delta t^{p2})$.

$$\begin{cases} \partial_t u + \partial_x(u^2) = \Delta_\alpha u, \quad 1 < \alpha \leqslant 2, \\ u(x,0) = 1/(2\cosh^2(x)), \end{cases} \tag{41}$$

where $u = u(x,t)$, $x \in \mathbb{R}$, and $t \in [0,T]$. Here, $u(x,0) = \partial_x v(x,0)$. The latter initial-value problem (41) is the fractal Burgers' equation which can be transformed into the fractal KPZ equation (40) via the substitution $u = \partial_x v$, taking into account the fact that the operators Δ_α and ∂_x commute. Fig. 10(a) shows the numerical solution of the fractal KPZ equation (40), while Fig. 10(b) shows the solution of the fractal Burgers' equa-

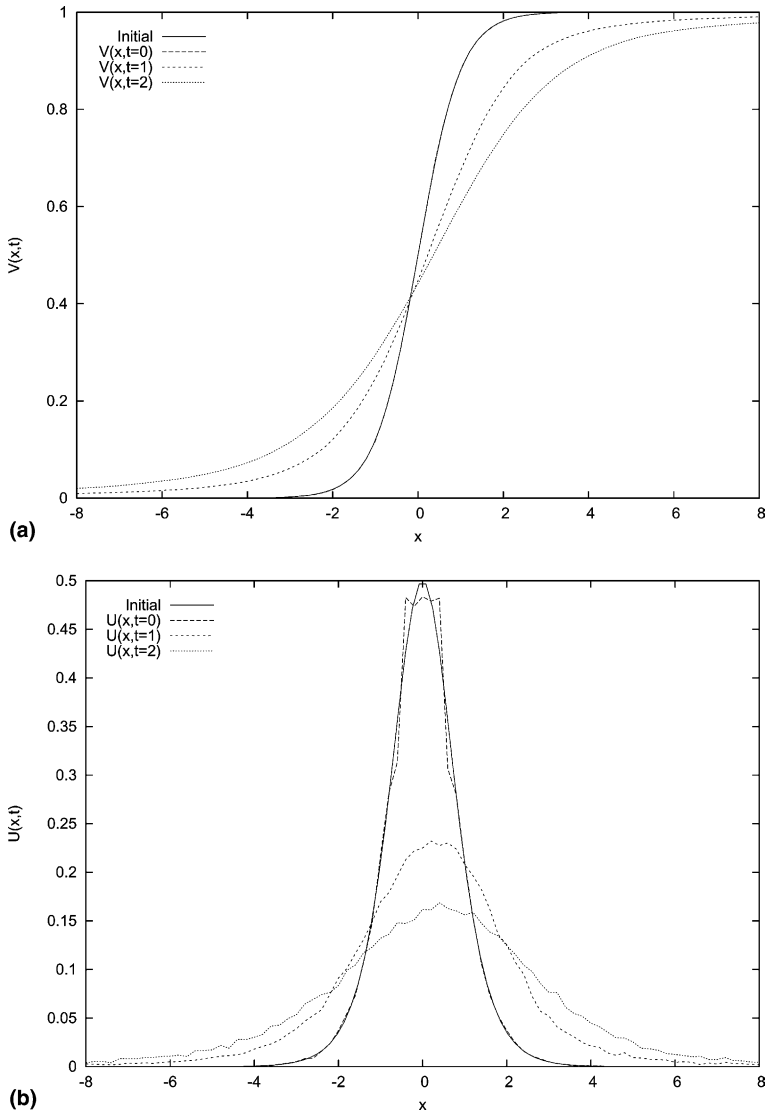

Fig. 10. Solutions constructed from the same interacting particles approximation using 50,000 particles at $t = 0$, 1, 2 for (a) the 1D fractal KPZ equation ($\alpha = 1.5$) (b) the 1D fractal Burgers' equation ($\alpha = 1.5$); the exact initial condition also plotted (full line).

tion (41). Both these solutions are obtained from the final state of the same system of particles by computing different statistics as discussed above.

5. Numerical experiments in two space dimensions

As is well known, Monte-Carlo simulations become increasingly attractive when the number of spatial dimensions increases. To show evidence regarding the flexibility and feasibility of these approximations, several numerical experiments in two space dimensions are presented here. For all the following simulations the initial condition is a two-dimensional Gaussian distribution.

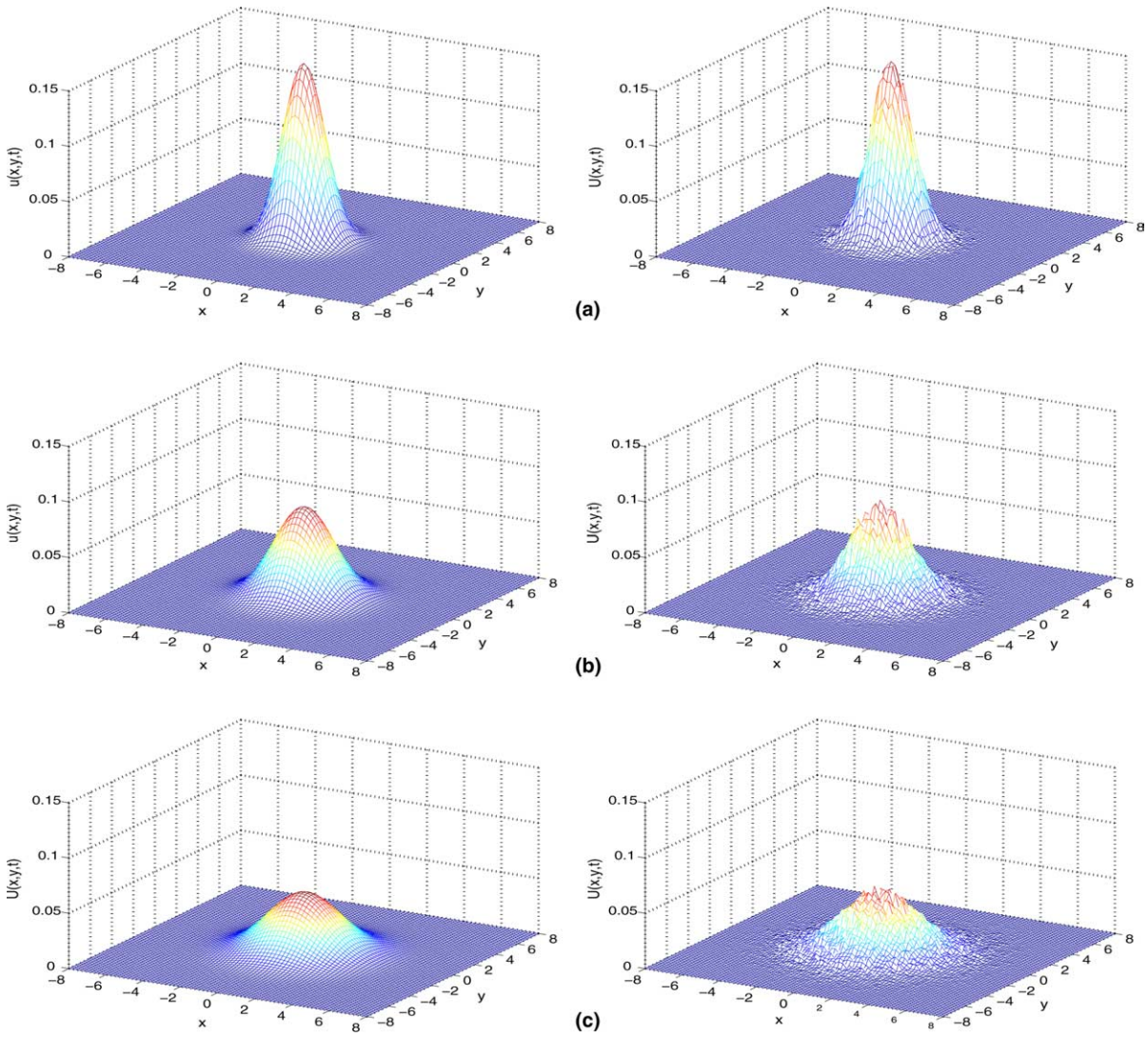

Fig. 11. Exact (left) and approximate (right) solution to the 2D incompressible Navier–Stokes equation in the vorticity formulation for (a) $t = 0.5$ (b) $t = 1$ (c) $t = 1.5$. $N = 120{,}000$ particles, smoothing parameter $\epsilon = 1.0$.

5.1. Navier–Stokes equation

Consider the vorticity formulation of the two-dimensional Navier–Stokes equations

$$\begin{cases} \partial_t u + \int_{\mathbb{R}^2} K(x-y)u(y,t)\,\mathrm{d}y \cdot \nabla u = \Delta u, \quad t \geqslant 1/2, \\ u(x_1,x_2,1/2) = 1/(2\pi)\exp\left(-\left(x_1^2+x_2^2\right)/2\right), \end{cases} \tag{42}$$

where $u = u(x_1,x_2,t)$, $(x_1,x_2) \in \mathbb{R}^2$, $t \in [1/2,T]$, and K is the Biot–Savart kernel (5). The initial condition $u(x_1,x_2,t = 1/2)$ corresponds to the exact solution

$$u(x_1,x_2,t) = \frac{1}{4\pi t}\exp\left(-\left(x_1^2+x_2^2\right)/4t\right)$$

representing an isolated vortex. Figs. 11 and 12 show the two-dimensional exact and approximate solution and cuts along two perpendicular planes through the origin, respectively. Table 6 presents numerical estimates of the L^2-norm of the absolute error in the approximate solution $U(x_1,x_2,T)$ at times $T = 0.5$, 1, 1.5, 2. Each discrete error is computed using the two-dimensional analogue of (32). It can be noticed that the errors are low despite the small number of particles, $N = 120{,}000$, used in the simulation.

5.2. Scalar Burgers' equation

For the case of anomalous diffusion we consider the scalar two-dimensional fractal Burgers' equation

$$\begin{cases} \partial_t u + u\partial_{x_1} u + u\partial_{x_2} u = \Delta_{1.5} u, \\ u(x_1,x_2,0) = 1/(2\pi)\exp\left(-\left(x_1^2+x_2^2\right)/2\right), \end{cases} \tag{43}$$

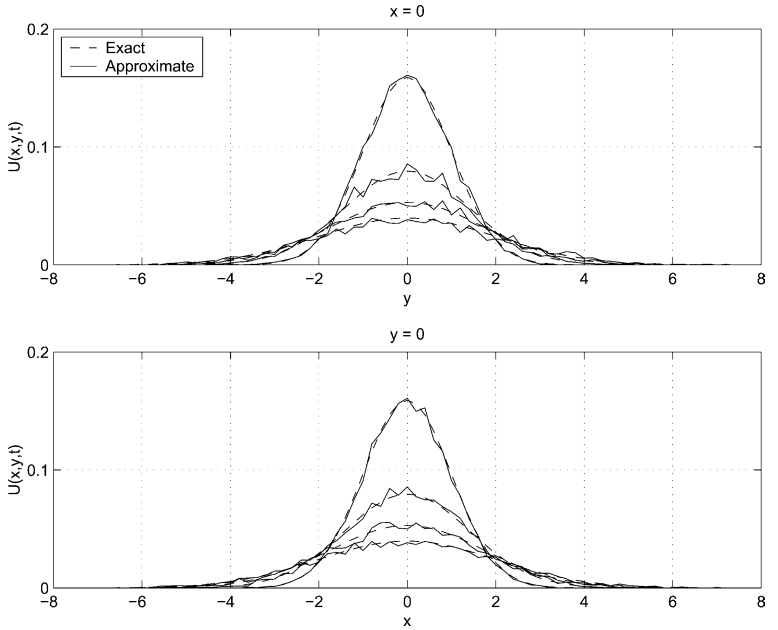

Fig. 12. The approximate versus the exact solution for the Navier–Stokes equation in two perpendicular planes through the origin at several times.

Table 6
Discrete errors for the 2D Navier–Stokes equation

T	0.5	1	1.5	2
$\|\text{error}\|_2$	8.8817e − 3	9.9515e − 3	9.6396e − 3	9.6660e − 3

where $u = u(x_1, x_2, t), (x_1,\ x_2) \in \mathbb{R}^2$, and $t \in [0, T]$. The solution is constructed using a system of $N = 600{,}000$ particles. Fig. 13 shows the exact and approximate initial condition as well as the shape of the solution at two later times. In Fig. 14, we show the solution along the $x = 0$ and $y = 0$ planes at several time instants. Furthermore, Fig. 15 plots the analytical estimated decay rate together with the estimate obtained from our numerical experiment for Eq. (31)

$$\|U(t)\|_2 \leqslant 0.90634(1+t)^{-2/3}.$$

5.3. Parallel implementation

Since a large number of particles are needed to generate an accurate solution, all our programs have been implemented in parallel. The parallel implementation is relatively straightforward and requires only a

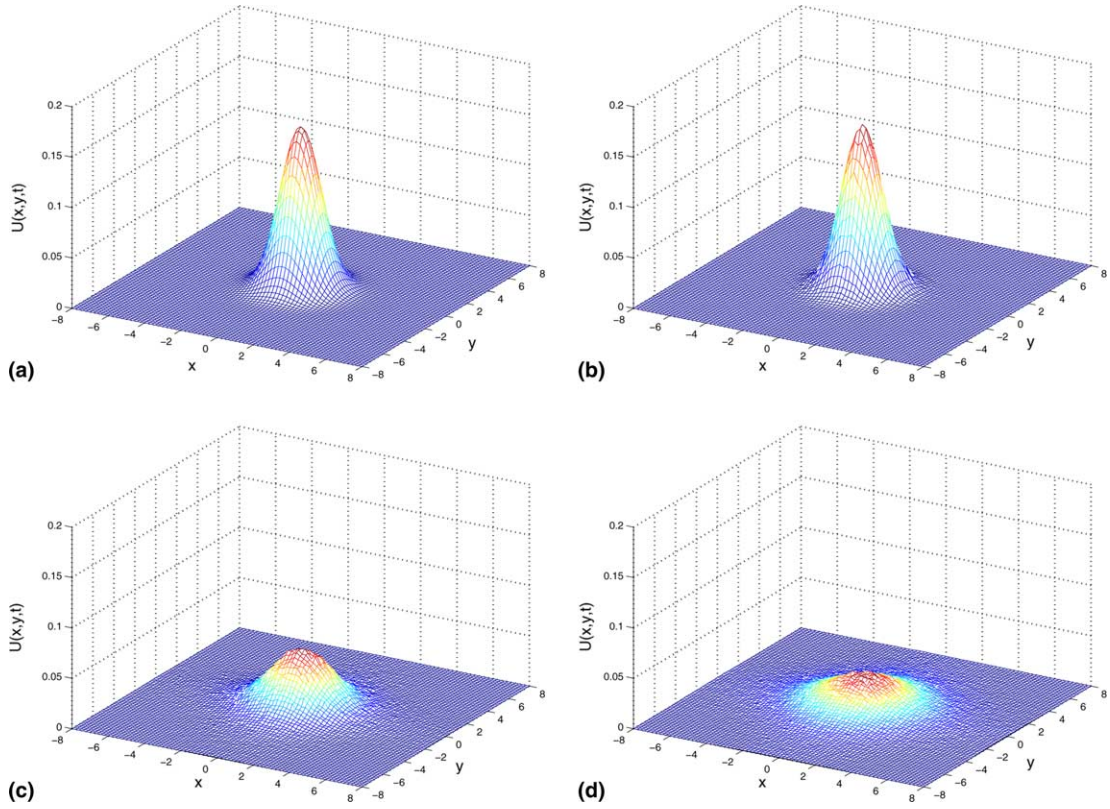

Fig. 13. Interacting particles approximation to the solution of the 2D fractal ($\alpha = 1.5$) Burgers' equation using 600,000 particles with the smoothing parameter $\epsilon = 1.0$. (a) Exact initial condition, (b) approximate initial condition, (c) approximation at $t = 0.5$, and (d) Approximation at $t = 1$.

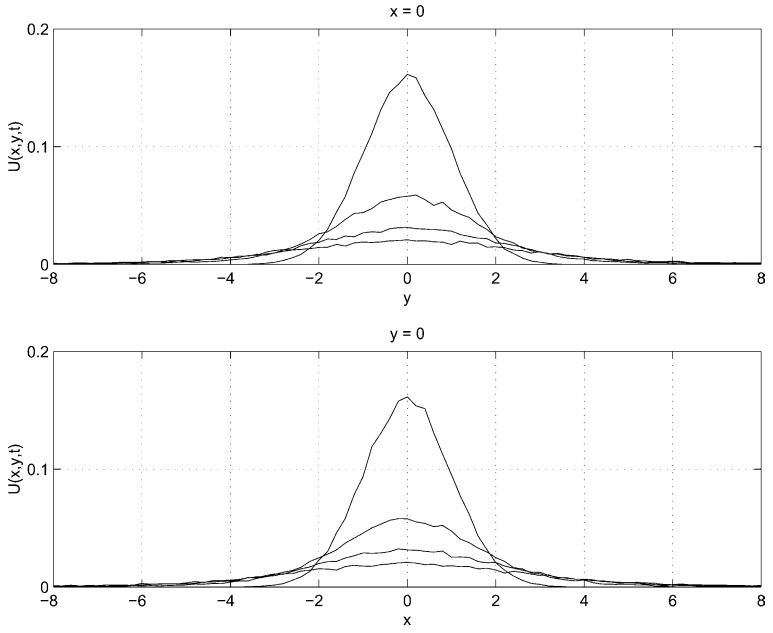

Fig. 14. Solution to the 2D fractal Burgers' equation in two perpendicular planes through the origin at several times.

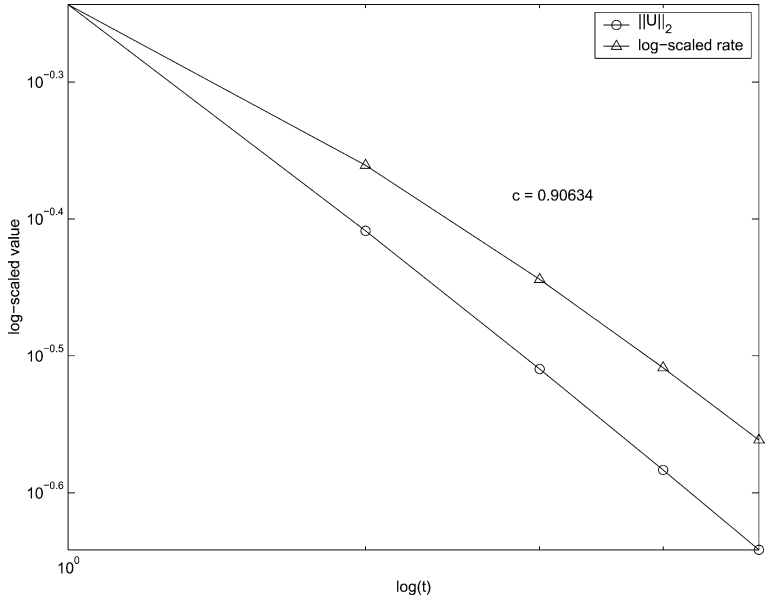

Fig. 15. Time decay of the solution to the 2D fractal ($\alpha = 1.5$) Burgers' equation using 600,000 particles.

global gathering of information per each time step for the particle position vector. The programs are written in Fortran using the portable communication library Message-Passing Interface (MPI) [22], under the Single Instruction Multiple Data paradigm. To run the examples, we used a cluster of SGI Origin200 machines with four processors per machine running at 175 MHz.

Acknowledgments

The support of Dongjin Kim through the NSF EPSCoR Grant EPS-9983278 is gratefully acknowledged. The numerical results were obtained using the computer resources of the Institute for Scientific Computation, part of which were acquired with support from the NSF DMS/Blue Cluster Grant 0421935.

References

[1] P.E. Kloeden, E. Platen, Numerical Solution of Stochastic Differential Equations, third ed., Springer, Berlin, 1999.
[2] P.E. Kloeden, E. Platen, H. Schurz, Numerical Solution of SDE through Computer Experiments, Springer, Berlin, 1997.
[3] H.J. Kushner, P. Dupuis, Numerical Methods for Stochastic Control Problems in Continuous Time, third ed., Springer, Berlin, 2000.
[4] G.N. Milstein, M.V. Tretyakov, Stochastic Numerics for Mathematical Physics, Springer, Berlin, 2004.
[5] B. Oksendal, Stochastic Differential Equations – An Introduction with Applications, sixth ed., Springer, Berlin, 2003.
[6] A.J. Chorin, Hermite expansions in Monte-Carlo computation, J. Comp. Phys. 8 (1971) 472–482.
[7] P. Biler, T. Funaki, W.A. Woyczynski, Interacting particle approximation for non-local quadratic evolution problems, Probab. Math. Stat. 19 (1999) 267–286.
[8] P. Biler, T. Funaki, W.A. Woyczynski, Fractal Burgers equations, J. Diff. Eq. 148 (1998) 9–46.
[9] P. Biler, W.A. Woyczynski, Global and exploding solutions for non-local quadratic evolution problems, SIAM J. Appl. Math. 59 (1998) 845–869.
[10] M. Kardar, G. Parisi, Y.-C. Zhang, Dynamic scaling of growing interfaces, Phys. Rev. Lett. 56 (1986) 889.
[11] J.A. Mann Jr., W.A. Woyczynski, Growing fractal interfaces in the presence of self-similar hopping surface diffusion, Physica A 291 (2001) 159–183.
[12] C. Canuto, M.Y. Hussaini, A. Quarteroni, T.A. Zang, Spectral Methods in Fluid Dynamics, Springer, Berlin, 1988.
[13] M. Bossy, D. Talay, A stochastic particle method for the McKean-Vlasov and the Burgers equation, Math. Comp. 66 (217) (1997) 157–192.
[14] M. Bossy, L. Fezoui, S. Piperno, Comparison of a stochastic particle method and a finite volume deterministic method applied to Burgers equation, Monte Carlo Meth. Appl. 3 (No. 2) (1997) 113–140.
[15] M. Bossy, D. Talay, Convergence rate for the approximation of the limit law of weakly interacting particles: application to the Burgers equation, Ann. Appl. Probab. 6 (No. 3) (1996) 818–861.
[16] A.S. Sznitman, Topics in propagation of chaos, in: P.L. Hennequin (Ed.), Ecole d'Eté de Probabilités de Sainy-Flour XIX – 1989, Lecture Notes in Mathematics, vol. 1464, Springer-Verlag, Berlin, 1991, pp. 165–251.
[17] J. Jacod, Sharp estimates for the Euler scheme for Lévy driven stochastic differential equations, Laboratoire de Probabilités et Modéles Aléatoires (CNRS UMR 7599) Université Pierre et Marie Curie, 2001. Available from: <http://www.proba.jussieu.fr/mathdoc/preprints/jj.Fri_May_11_14_17_15_CEST_2001.html>.
[18] P. Protter, D. Talay, The Euler scheme for Lévy driven stochastic differential equations, Ann. Probab. 25 (No. 1) (1997) 393–423.
[19] G. Samorodnitsky, M.S. Taqqu, Stable Non-Gaussian Random Processes – Stochastic Models with Infinite Variance, Chapman & Hall/CRC, London, 1994.
[20] R.N. Mantegna, Fast, accurate algorithm for numerical simulation of Lévy stable stochastic processes, Phys. Rev. E 49 (1994) 4677–4683.
[21] J.M. Chambers, C. Mallows, B.W. Stuck, A method for simulating stable random variables, J. Am. Stat. Assoc. 71 (1976) 340–344.
[22] W. Gropp, E. Lusk, A. Skjellum, Using MPI: Portable Parallel Programming with the Message-Passing Interface, The MIT Press, 1994.